Article

Research on Four-channel Wide Dynamic Microwave Rectifier with a Shared Load

Cheng Peng [1,2]*, Zhihao Ye [1], Biao Zhao [2] ,Han Xiao[1] and Zerun Wang[1]

[1] Naval University of Engineering, Wuhan 430000, China
[2] National University of Defense Technology, Wuhan, 430000, China
* Correspondence: aul0421@sina.com.cn

Abstract: This paper has designed a four-channel wide dynamic microwave rectifier circuit for the shortcomings of uneven output voltage of each branch of the multi-channel rectification technology. A voltage-doubling rectifier circuit with identical structure was used in each branch. The four rectifier branches shared the same load at the output terminal, allowing the rectifier circuit to have an RF-DC conversion efficiency greater than 50% over the input power range from 12mW to 274mW, widened by 274% compared to a single channel. Not only the advantages of multi-channel technology with wide dynamics were retained, but also the output voltage was highly consistent and could be directly output in parallel without complex power electronics conversion.

Keywords: shared load; four-channel; wide dynamic; microwave rectification

1. Introduction

Since Dr. Peter Grasher proposed the concept of satellite solar Power Station (SPS) [1-3], radio energy transmission technology, especially Microwave Wireless Power Transfer (MWPT) technology, has gradually attracted people's attention. Figure 1 shows the MWPT schematic diagram. Due to the use of 300MHz-300GHzAs the carrier of energy transmission, MWPT has the advantages of long transmission distance and large transmission power compared with other wireless transmission methods [4-6]. Of course, MWPT technology also has some shortcomings. Firstly, the overall energy conversion efficiency of DC-DC in MWPT system is still at a low level with the current technological level. Although the energy conversion efficiency of DC-RF at the transmitter and RF-DC at the receiver can reach more than 70% under ideal conditions, However, due to the influence of various factors such as antenna performance and transmission environment during electromagnetic wave space transmission, the power Pin (dBm) reaching the receiving end is extremely unstable and has a wide dynamic range [7].When the input power changes, the nonlinearity of the rectifier device will correspondingly change the impedance in the input terminal, which leads to an impedance mismatch and greatly reduces the rectification efficiency [8]. Therefore, many scholars have focused on the wide dynamic rectification technology. Most of the current wide dynamic rectification technology use multi-channel technology. For example, some scholars have designed a two-way adaptive control rectifier circuit by the sensitivity of MOSFETs to voltage. The power operating range of the circuit was broadened by switching the field-effect tube control circuit in two states, namely, series and parallel [9-11]. Some scholars have also used microwave passive networks, such as non-uniform Wilkinson power dividers, to fully utilize the rectification capability of both high and low power branches, thus broadening the overall rectification capability of the circuit [12-15]. Based on the two-way microwave rectifier circuit, the research team of South China University of Technology introduced a third microwave rectifier circuit. The energy reflected from the first two branches due to impedance mismatch was fed to the third rectifier branch through a directional coupler, which significantly broadened the overall power dynamic range of the three-way output [16-19].

Preprints (www.preprints.org) | NOT PEER-REVIEWED | Posted: 16 June 2023 doi:10.20944/preprints202306.1204.v1

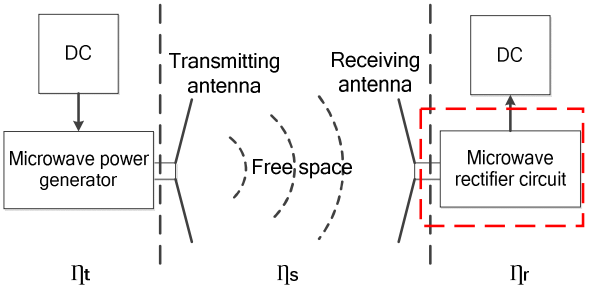

Figure 1. MWPT schematic diagram

The non-uniform power distribution or automatic power distribution can effectively broaden the power dynamic range of microwave rectifier circuits and improve the stability of rectification efficiency of microwave rectifier circuits in the case of unstable spatial transmission. However, since each rectification branch in these two methods is non-uniform, the DC voltage at the output terminal of each branch is different and cannot be directly connected in parallel to charge the battery. A complex power electronic converter circuit (boost or buck circuit) needs to be introduced to adjust the output voltage of each branch to be consistent before parallel output. This results in additional power loss and is not conducive to DC power synthesis at the output load terminal. In order to solve this problem, it becomes necessary to study multi-channel rectifier circuits with consistent output voltages. Such a circuit will not only broaden the power dynamic range of the rectifier circuit, but also enable the output voltage to be directly used for battery charging in parallel, avoiding complex power electronic conversion at the load side that will influence the wireless charging efficiency. Therefore, this circuit has high practical value. To obtain a wide dynamic rectifier circuit that facilitates DC power synthesis at the output terminal, a four-channel wide dynamic microwave rectifier circuit has been designed in the paper for the shortcomings of the traditional wide dynamic rectifier circuit with uneven output voltage. The four rectifier branches shared the same load at the output terminal, allowing the rectifier circuit to have an RF-DC conversion efficiency greater than 50% over the input power range from 12mW to 274mW, widened by 274% compared to a single channel. Not only the advantages of multi-channel technology with wide dynamics were retained, but also the output voltage was highly consistent and could be directly output in parallel without complex power electronics conversion. To a certain extent, the output power and the practicality of this energy harvesting system have been increased. Finally, a complete MWPT experimental system was built, and the experimental results proved the feasibility of the scheme.

2. Analysis of the principle of the circuit

2.1. Combination form of multi-channel rectification

The combined form of the multi-channel rectifier circuit is shown in Fig. 2. Fig. 2(a) shows that the electromagnetic waves in space were collected by each antenna unit of the antenna array, transformed into RF power all the way through the combiner, delivered to a conventional single-channel rectifier circuit, and then converted into DC voltage output at the load side. Although the use of antenna arrays allowed for greater input power, a conventional single channel was used in the rectifier circuit, which had a narrow power dynamic range. In Fig. 2(b), multiple antennas were used for diversity reception, and each antenna unit corresponded to an independent rectifier circuit, which can ensure that multiple channels could harvest energy simultaneously with a wide power dynamic range. However, since the antennas were located in different locations in space, it was impossible to guarantee that each antenna got the same power. Even if the performance of each rectifier branch was the same, it was difficult to make each output voltage consistent, and the output side should be equipped with a boost or buck circuit in order to output stable voltage in parallel. These circuits themselves introduced losses that influenced the efficiency of the DC synthesis output at the load

Preprints (www.preprints.org) | NOT PEER-REVIEWED | Posted: 16 June 2023 doi:10.20944/preprints202306.1204.v1

terminal. In this paper, the form of Fig. 2(c) was used. The electromagnetic energy received by each unit of the antenna array was combined and input to the quartile power distribution network, and output to four identical voltage doubling rectifier circuits respectively. Such a multi-channel rectification technology not only increased the power capacity of the rectifier circuit and broadened the power dynamic range, but also enabled each circuit to obtain a high and consistent output voltage. In this way, the outputs can be directly connected in parallel for battery charging, avoiding the need for complex power electronic transformations and thus maintaining stable DC synthesis output efficiency.

As shown in Fig. 2(c), the RF power obtained from each antenna unit of the high-gain antenna array was combined into one RF power P_{in} input to the rectifier circuit through the combiner, thus a good input power could be obtained. At the output side, the output voltage of each branch was equal and all rectifier branches shared the same load Z_{load}. In this way, not only can a larger DC output power be obtained, but it could also be used to charge the battery directly. The characteristics of the circuit can be expressed by the following equation:

$$P_{in} = P_{in1} + P_{in2} + P_{in3} \cdots + P_{inN} \quad (1)$$

$$V_{out} = V_1 = V_2 = V_3 \cdots = V_N \quad (2)$$

$$I_1 = I_2 = I_3 \cdots = I_N \quad (3)$$

$$Z_1 = Z_2 = Z_3 \cdots = Z_N \quad (4)$$

$$I_{out} = I_1 + I_2 + I_3 \cdots + I_N \quad (5)$$

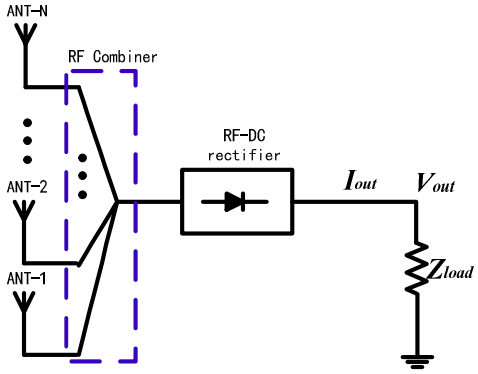

(a) Multi-antenna combiner-single-channel microwave energy harvesting

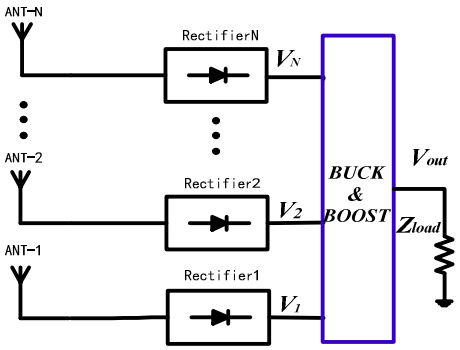

(b) Multi-antenna diversity reception - multi-channel rectified output

Preprints (www.preprints.org) | NOT PEER-REVIEWED | Posted: 16 June 2023 doi:10.20944/preprints202306.1204.v1

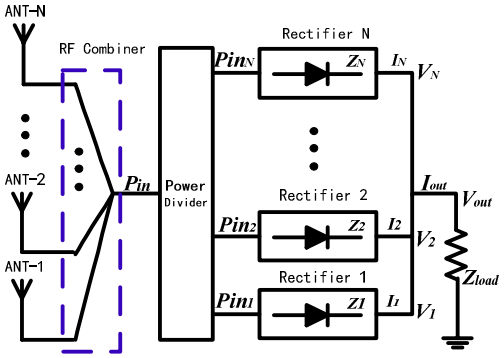

(c) Multi-antenna combiner - multi-channel rectified output

Figure 2. Structure of several multi-channel microwave energy harvesting circuits

In fact, for each rectifier branch, the output impedance was equal. According to the above formula, the DC output power at the load can be derived as:

$$P_{DC} = \frac{V_{out}^2}{Z_{load}} = I_{out}^2 \cdot Z_{load} \quad (6)$$

The overall efficiency of the circuit can be expressed as:

$$P_{CE} = \frac{P_{DC}}{P_{in}} \times 100\% \quad (7)$$

2.2. Mechanisms for achieving wide power dynamic range

Taking a four-channel microwave rectifier circuit with equal power division as an example, this paper has analyzed the effect of multi-channel rectification on the power dynamic range by establishing an approximate mathematical model based on the interval. It was still assumed that the power dynamic range of a single rectifier branch was approximated as a equilateral triangle. Since it was 1 divided into 4 uniform distribution, we could assume each branch input power $P_1=P_2=P_3=P_4=x$, then the total input power $P_{in}=4x$. As shown in Fig. 3, the single branch rectification efficiency greater than 50% was in the interval of [1.5W,2.5W] with a dynamic range of 1W. All four rectifier branches had the same form. The power dynamic range of the combined four-channel rectifier circuit was shown in the Fig., and its total efficiency above 50% was between [6W,10W] with a dynamic range of 4W, which was four times that of the single rectifier branch.

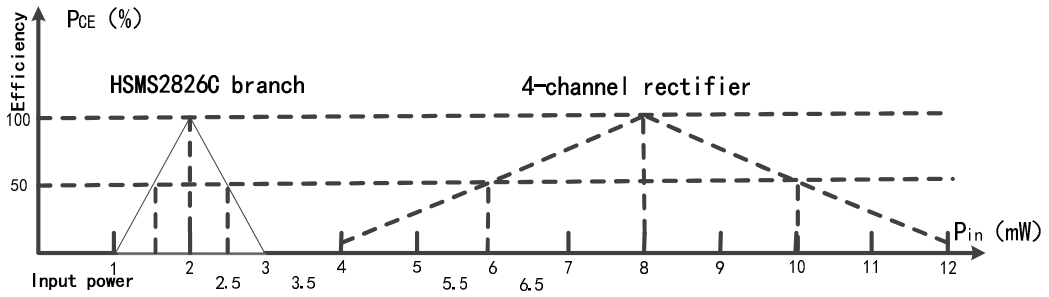

Figure 3. Equivalent mathematical model of four-channel wide dynamic microwave rectifier circuit

Preprints (www.preprints.org) | NOT PEER-REVIEWED | Posted: 16 June 2023 doi:10.20944/preprints202306.1204.v1

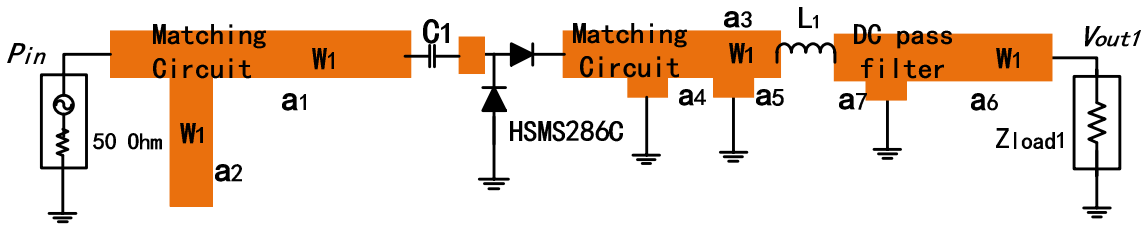

Figure 4. Circuit structure of a single rectifier branch

Ideally, multi-channel rectification technology can broaden the power dynamic range of RF-DC energy conversion, the fundamental reason of which is that it can broaden the power "capacity" of the rectifier circuit. That is, it allows more RF power to be converted to DC energy through the rectifier circuit at the same time.

3. Simulation and design of the circuit

3.1. Design of single-circuit microwave rectifier circuit

Before designing the four-channel rectifier circuit, the single-channel microwave rectifier circuit first needs to be designed on the simulation software. The HSMS286C voltage doubling rectifier structure was used, and a low-pass filter with a simple structure was used as the DC filter. After simulation optimization, the structure of a single rectifier branch was obtained as shown in Fig. 4. The dielectric constant of the plate was ε_r and the thickness of the plate was H. At the operating frequency of 2.45 GHz, the microstrip antenna width was W_1, the length of front impedance matching series branch was a_1, the parallel branch length was a_2, the length of rear impedance matching series branch was a_3, the length of parallel short circuit branch was a_4、a_5, the series inductor was L_1, the length of DC filter series branch was a_6, the parallel branch length was a_7, and the load was Z_{load1}. After optimization, the parameters of each circuit are shown in Table 1.

Table 1. Single-branch microwave rectifier circuit

Parameter	Value
ε_r	2.65
H	0.762mm
W_1	2.08mm
a_1	28.1mm
a_2	11.4mm
a_3	6.5mm
a_4	1mm
a_5	1mm
a_6	6mm
a_7	1mm
C_1	100pF
L_1	100nH

In order to better analyze the variation law of output DC voltage with input power, the parameters of individual rectifier branch S_{11} and the variation curve of output DC voltage V_{out1} with input power P_{in1} were obtained by software simulation. From the S curve in Fig. 5(a), it can be seen that when P_{in1} was between the power interval of 0dBm to 23dBm, S_{11} was less than -10dB, indicating that the branch was in a better impedance matching state in this interval. And from the output voltage curve in Fig. 5(b), it can be seen that as the input power gradually increased from P_{in1} = 5dBm, the slope of the voltage increased with power, and the output voltage V_{out1} also gradually increased. When P_{in1}=16dBm, the slope of the increment of V_{out1} was maximum, which was 3.8V. When the input

Preprints (www.preprints.org) | NOT PEER-REVIEWED | Posted: 16 June 2023 doi:10.20944/preprints202306.1204.v1

power P_{in1} exceeded 20dBm, although the output voltage V_{out1} was still increasing, it increased slowly and gradually entered a stable status. Since the load was constant, it indicated that the increased input power did not bring enough output power. This was because the diode was reversed breakdown, which caused additional power loss, and the RF-DC rectification efficiency started to drop.

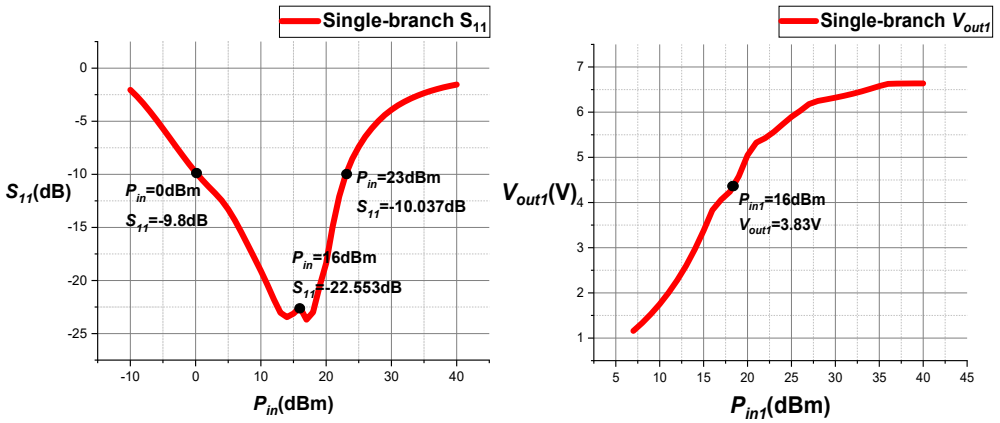

(a)S11-Pin1 curve (b)Vout1-Pin1 curve

Figure 5. The variation curve of S11 and Vout1 with input power

Let the input power of a single rectifier branch be P_{in1} (unit was dBm) as a variable, the real part of the output voltage was V_{out1} (unit was V), Z_{load1} was the load impedance of the branch, the single microwave rectifier branch RF-DC conversion efficiency P_{CE1} (Power Conversion Efficiency, PCE1) could be calculated according to the following formula:

$$P_{CE1} = \frac{1000 \cdot V_{out1}^2 / Z_{load1}}{10^{P_{in1}/10}} \times 100\% \quad (7)$$

To further illustrate the power dynamic range of this rectifier, the efficiency-input power dynamic range curve for a single rectifier branch was plotted in Fig. 6. The curve shows that the maximum rectification efficiency of a single rectifier branch appeared when the input power P_{in1} = 16dBm, the maximum RF-DC conversion efficiency at this time was 72.27%. It can also be seen from the curve that for a single branch input power P_{in1} between 6dBm to 20dBm (about 14dBm power dynamic range), the RF-DC conversion efficiencies were all greater than 50%.

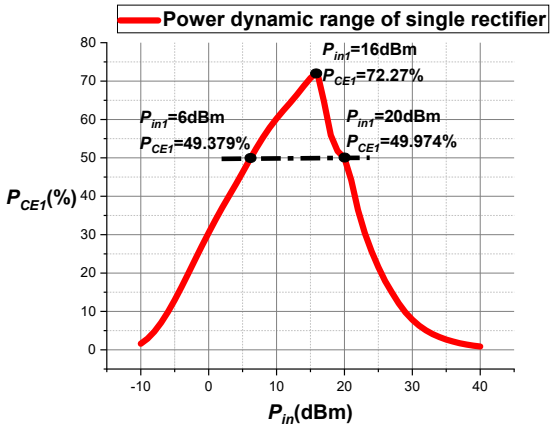

Figure 6. Power dynamic range of a single rectifier branch

3.2. Design of quadratic power division network

Preprints (www.preprints.org) | NOT PEER-REVIEWED | Posted: 16 June 2023 doi:10.20944/preprints202306.1204.v1

According to the principle of Wilkinson power divider, when certain conditions are met, the power divider can divide the input RF power equally into two branches for output. By nesting three such equally divided Wilkinson power dividers together, a four-equivalent network was obtained. As shown in Fig. 7, the board material dielectric constant was ε_r, the thickness of the plate was H, the width of the power divider transmission line was W_0, the width of the 1/4 wavelength converter was W_{02}, and the isolation resistance was R. Simulation and optimization of this power-division network were carried out to obtain the parameters of the power-division network circuit, as shown in Table 2.

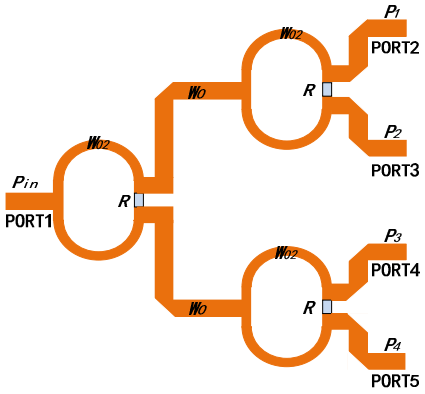

Figure 7. Schematic diagram of the structure of the four-equivalent power division network

Table 2. List of circuit parameters of the four-equivalent power divider

Parameter	Value
ε_r	2.65
H	0.762mm
W_0	2.03mm
W_{02}	1.1173mm
R	100Ohm

The S parameters of the designed four-equivalent Wilkinson power divider network were simulated, and the S-parameter characteristic curves of each port are shown in Fig. 8. As can be seen in Fig. 8, the power-division network S11 = -26.5 dBm at 2.45 GHz and maintains impedance matching over a wide bandwidth range. Each output port S_{21}、S_{31}、S_{41}、S_{51} were highly overlapping, and S_{21}=S_{31}=S_{41}=S_{51}≈-6dB at 2.45GHz. This indicated that the power at each output port was 1/4 of the input power P_{in}, and the RF input power obtained from the antenna by the rectifier circuit had been evenly divided into four equal-sized portions.

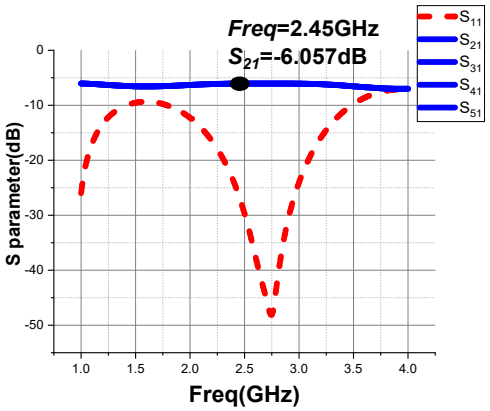

Figure 8. S-parameter simulation of the four-equivalent power division network structure

Preprints (www.preprints.org) | NOT PEER-REVIEWED | Posted: 16 June 2023 doi:10.20944/preprints202306.1204.v1

3.3. Overall circuit performance optimization and analysis

As shown in Fig. 9, four identical single rectifier circuits were connected to the four output interfaces of the four-equivalent power divider network, and the whole four-channel microwave rectifier circuit was simulated and optimized. Its general parameters were consistent with those of individual debugging. Due to the change of parameters after the circuit combination, the microstrip line length at the load side and the parameters of the load Z_{load} itself needed to be optimized, and the optimized circuit parameters are shown in Table 3.

Table 3. Overall parameters of the circuit

Parameter	Value
Z_{load}	180Ω
$W1$	2.08mm
a_8	18.59mm
a_9	8.84mm
a_{10}	9mm
a_{11}	5mm

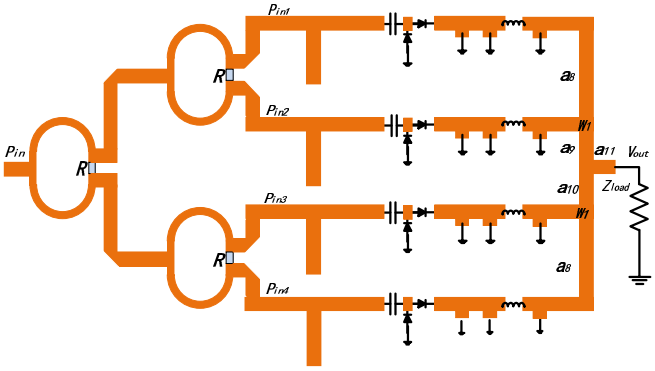

Figure 9. The overall structure of the four-channel rectifier circuit

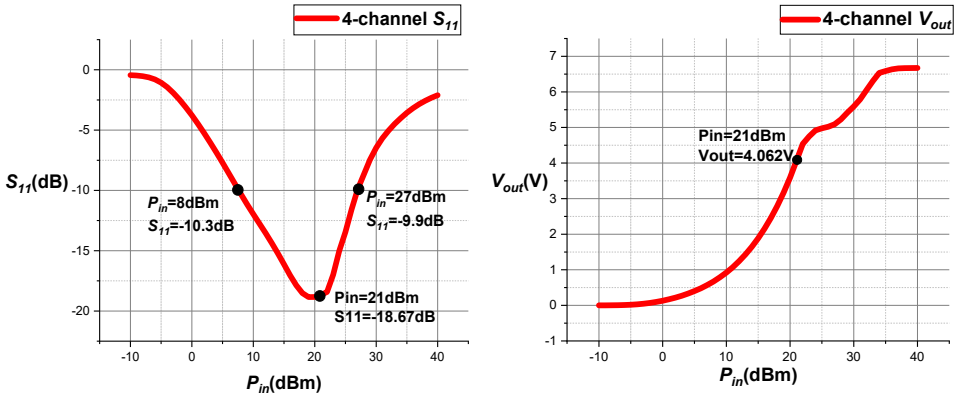

(a)S11-Pin curve (b)Vout-Pin curve

Figure 10. Variation curve of S11/Vout with Pin

The S_{11} parameter of the whole rectifier circuit and the variation curve of the output DC voltage V_{out} with the input power P_{in} were obtained by software simulation. From the S curve in Fig. 10 (a), it could be seen that when P_{in} was between the interval of 8dBm to 27dBm, S11 was less than -10dB, indicating that the branch was in a better impedance matching state in this interval. When the input power P_{in} = 21dBm, S_{11}= -18.67dB. And as can be seen from the output voltage curve in Fig. 10(b), as the input power gradually increased from P_{in} = -10dBm, the slope of the voltage increased with power,

Preprints (www.preprints.org) | NOT PEER-REVIEWED | Posted: 16 June 2023 doi:10.20944/preprints202306.1204.v1

and the output voltage V_{out} gradually increased. When P_{in} = 21dBm, the slope of the increment of V_{out} was maximum, at which time the output DC voltage was 4.062V. When the input power P_{in} exceeded 21dBm, the output voltage V_{out} increased slowly and gradually entered a stable status.

In this paper, the power dynamic range of the combined four-channel microwave rectifier circuit was compared with the power dynamic range of a single rectifier branch in Fig. 11. Fig. 11(a) shows a comparison of the power dynamic range in milliwatts. It can be seen that the RF-DC conversion efficiency of the designed four-channel microwave rectifier circuit with a shared load was greater than 50% when the input power P_{in} was in the range of 11dBm to 24dBm (a total range of 13dBm). Compared to the power from 6dBm to 19dBm in the single-channel rectifier, the range was not significantly broadened. However, the power capacity of the entire rectifier circuit was increased, making the rectifier circuit adapt to a wider input power range. If the input power P_{in} is converted into milliwatts, it can be seen that the RF-DC conversion efficiency of the four-channel rectifier is greater than 50% in the range of 12mW to 274mW (a total range of 262mW), which is much wider than the dynamic power range of 2mW to 72mW (only 70mW) for a single-channel microwave rectifier circuit.

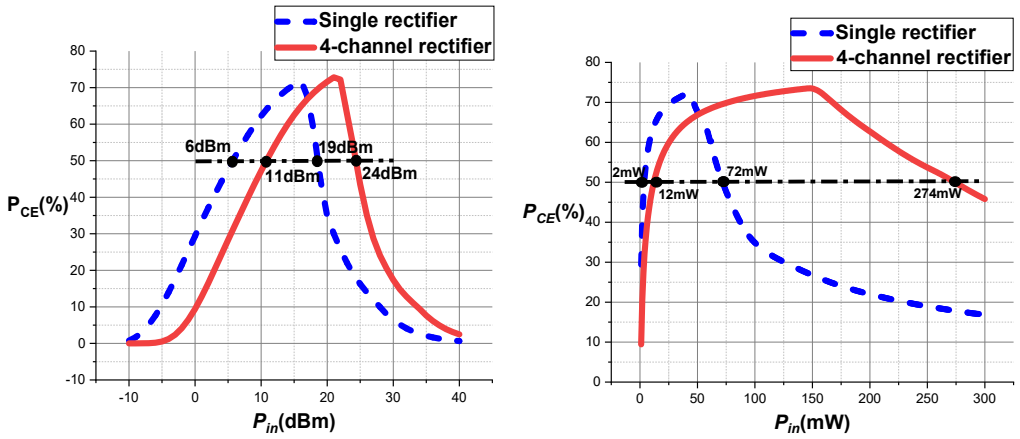

(a) Comparison of power dynamic range in dBm (b) Comparison of power dynamic range in mW

Figure 11. Comparison of Four-channel/single-channel power dynamic range

4. Experimental verification

4.1. Microwave rectifier circuit conduction experiment

The rectifier circuit was physically fabricated according to the circuit parameters of the simulation design, as shown in Fig. 12. Due to the uncertainty of spatial transmission, the input power P_{in} of the rectifier circuit could not be guaranteed to be constant. Therefore, the output voltage at the load side could also not be guaranteed to be a constant value. The charging of NiMH batteries generally requires a constant voltage to ensure safety. Therefore, a 1.5V regulator circuit was set up at the output, and a battery box was fixed on the circuit board. For wireless charging, a NiMH battery with a charging voltage of 1.5V could be loaded, with the positive terminal of the battery connected to a constant voltage output and the negative terminal grounded. Closed-loop conduction experiments were conducted on the designed circuit, and an RF signal generator was used as the microwave source. By adjusting the transmitting power of the microwave source, the output voltage V_{out} was recorded at the output load terminal. The charging voltage V_{charge} = 1.5V could be obtained by measuring the output of the voltage regulator circuit (positive and negative terminals of the battery).

Preprints (www.preprints.org) | NOT PEER-REVIEWED | Posted: 16 June 2023 doi:10.20944/preprints202306.1204.v1

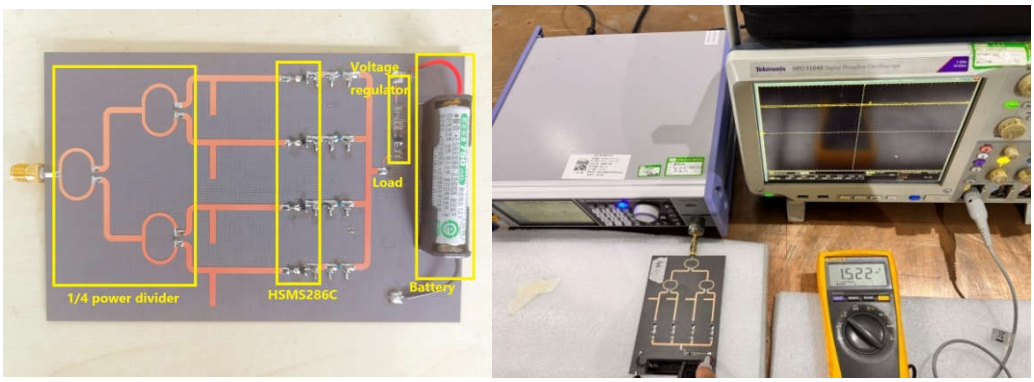

(a) Physical circuit (b) Test environment of the experiment

Figure 12. Rectifier circuit conduction experiment

In this paper, the power of the RF generator was set to 20dBm, and the output voltage at the load side and the regulated output voltage were measured respectively, as shown in Fig. 13. When the input power P_{in} = 20dBm (about 100mW) with 125 picoseconds as the sampling period to observe the output voltage situation, it could be seen in Fig. 13 (c) that the output voltage at the load side was about 2.04V, and be stabilized around 1.5V through the regulator circuit. This indicated that the circuit had successfully implemented a four-channel microwave rectifier to convert the RF signal to DC output with an RF-DC conversion efficiency of nearly 40%.

(a) Time domain waveform of voltage before voltage regulation

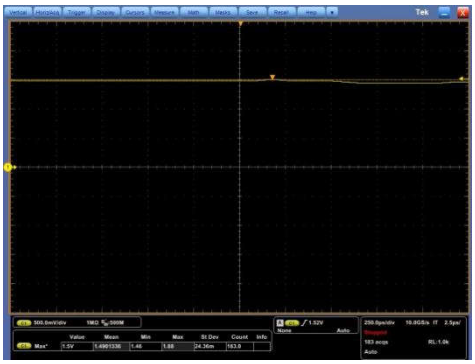

(b) Time domain waveform of voltage after voltage regulation

Preprints (www.preprints.org) | NOT PEER-REVIEWED | Posted: 16 June 2023 doi:10.20944/preprints202306.1204.v1

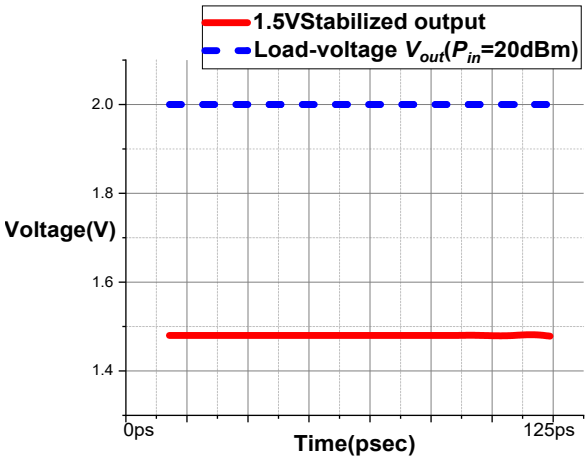

(c) Time domain waveform comparison before/ after the output voltage is regulated (125 picosecond sampling)

Figure 13. Voltage waveform at the output terminal in the rectifier circuit conduction experiment

4.2. Long-range wireless charging experiment

The designed four-channel microwave rectifier circuit was connected to the space transmission platform. In order to obtain better spatial transmission effect, the transmitting and receiving antennas all used 16-element circularly polarized antenna array, and were fixed by antenna brackets as well as 3D printed molded fasteners. The height of the transmitting and receiving antenna was 1.5 meters, and the distance between antennas was 3 meters. Keysight's 9310A microwave signal source was used as the RF transmitter, together with an amplifier as the microwave radiation source. The measured radiation power used in this experiment was 46dBm (about 40W) and the receiving antenna output power was 20dBm, as shown in Fig. 14.

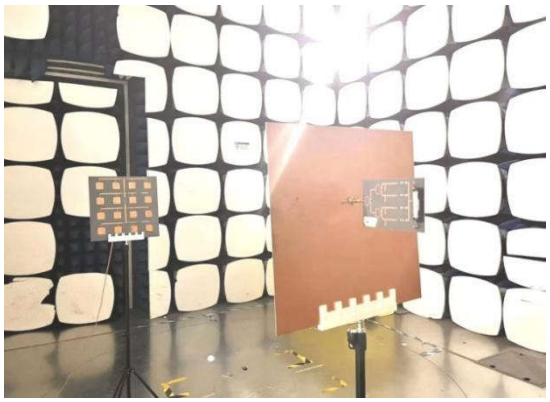

Figure 14. Long-range microwave wireless charging experiment

After fully discharging the Panasonic HHR-4MRC No.7 NiMH battery, it was put into the battery box of the rectifier circuit. By using the above spatial transmission scheme, the battery voltage before and after charging was measured and compared after irradiating the receiving antenna for a period of time, as shown in Fig. 15. Before charging, the battery was empty and the measured voltage was 0.82 V. After 1 hour of wireless charging, the battery power was obviously restored and the measured voltage was about 1.195 V. After about 1.5 hours, the voltage stabilized at about 1.45V, indicating that the battery had been fully charged. This proved that the MWPT system successfully completed long-range wireless charging at a distance of 3 meters, which can meet the charging requirements of some small wearable devices (e.g., cell phones, etc.) indoors.

Preprints (www.preprints.org) | NOT PEER-REVIEWED | Posted: 16 June 2023 doi:10.20944/preprints202306.1204.v1

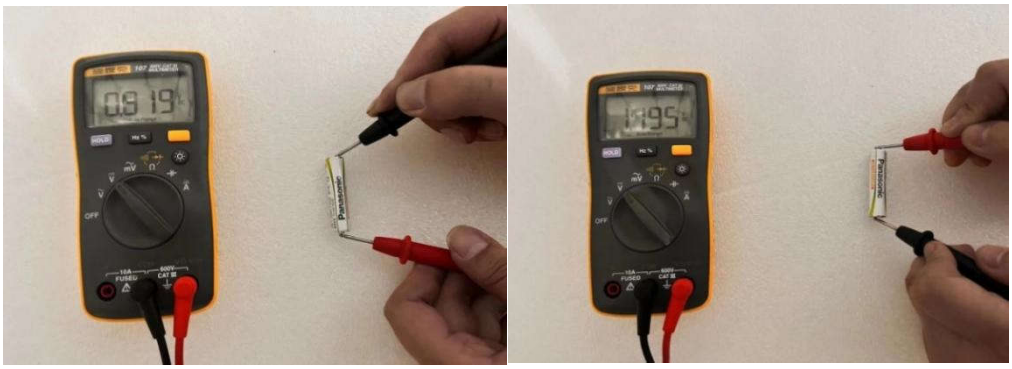

(a) Battery voltage before charging (b) Battery voltage after 1 hour of charging

(c) Powering the flashlight with the recharged battery

Figure 15. Comparison of battery voltage before/after charging

5. Conclusion

Because the input impedance of the schottky diode to the input power is relatively sensitive, so a single channel of the rectifier circuit of power dynamic range and capacity of the power is limited, multi-path technology is often used to broaden the power dynamic range of the microwave rectifier circuit, but the rectifier channels tend to be uneven, this paper designed a model for this problem more practical microwave rectifier circuit, First each branch using the same structure, sharing one load on the output side, this design has two advantages, one is to improve the output voltage, help the weak electromagnetic energy collection, 2 it is multiple rectifier branch in DC power output can be directly synthesis, without introducing the complex power electronic transformation, which can improve the charging efficiency. This structure facilitates direct DC power synthesis at the load side. the rectifier circuit to have an RF-DC conversion efficiency greater than 50% over the input power range from 12mW to 274mW, widened by 274% compared to a single channel. A complete MWPT experimental system was built, and this rectifier circuit structure was used to achieve microwave energy collection and storage through a 16-elements CP array at a distance of 3 meters.

References

[1] Brown, W.C. The history of power transmission by radio waves. *IEEE Trans. Microwave Theory Tech.* **1984**, *32*, 1230-1242.

[2] Sivagnanam, G.; Priya, P.L.; Sowmya, P.; Mathivanan, G.P. Wireless power transmission using inductive coupling. *Prgramm. Dev. Circuit. Syst.* **2012**, *4*, 260-263.

[3] Petersen, E.; Hansen, J.F. Self-tuning resonant power transfer systems. United States Patent 9287040, Pleasanton, CA, US, 2016.

[4] Cheng, S.; Chen, X.; Wang, J.; Wen, J.; J. Li. Key technologies and applications of wireless power transmission. *Trans. China Electrotech. Soc.* **2015**, *30*, 68-84.

[5] Fan, X.; Gao, L.; Mo, X.; Zhao, Q.; Jia, E. Overview of research status and application of wireless power transmission technology. *Trans. China Electrotech. Soc.* **2019**, *34*, 1353-1380.

[6] Xue, F.; Liu, S.; Kong, X. Single-layer high-gain flat lens antenna based on the focusing gradient metasurface. *Int. J. RF Microw. C. E.* **2020**, *30*, e22183.

[7] Peng, C.; Ye, Z.-H.; Xia, Y.-H.; Yang, C. Analysis on space transmission model of the Microwave Wireless Power Transfer system. *Frequenz* **2021**, *75*, 449-458.

[8] Wang, M.; Yang, L.; Fan, Y.; Shen, M.; Li, Y.; Shi, Y. A compact omnidirectional dual-circinal rectenna for 2.45 GHz wireless power transfer. *Int. J. RF Microw. C. E.* **2019**, *29*, e21625.

[9] Liu, Z.; Zhong, Z.; Guo, Y.-X. Enhanced dual-band ambient RF energy harvesting with ultra-wide power range. *IEEE Mirow. Wirel. Co.* **2015**, *25*, 630-632.

[10] Niotaki, K.; Georgiadis, A.; Collado, A.; Vardakas, J.S. Dual-band resistance compression networks for improved rectifier performance. *IEEE Trans. Microw. Theory* **2014**, *62*, 3512-3521.

[11] Zhang, X.Y.; Lin, Q.-W. High-efficiency rectifier with extended input power range based on two parallel sub-rectifying circuits. In Proceedings of 2015 IEEE International Wireless Symposium (IWS 2015), Shenzhen, China, 30 March-1 April 2015; pp. 1-4.

[12] Peng, C.; Ye, Z.; Wu, J.; Chen, C.; Wang, Z. Design of a Wide-Dynamic RF-DC Rectifier Circuit Based on an Unequal Wilkinson Power Divider. *Electronics* **2021**, *10*, 2815.

[13] Zhang, L.; Ji, S.; Gu, S.; Huang, X.; Palmer, J.E.; Giewont, W.; Wang, F.F.; Tolbert, L.M. Design considerations for high-voltage insulated gate drive power supply for 10-kV SiC MOSFET applied in medium-voltage converter. *IEEE Trans. Ind. Electron.* **2020**, *68*, 5712-5724.

[14] Zhang, L.; Ruan, X. Control schemes for reducing second harmonic current in two-stage single-phase converter: An overview from DC-bus port-impedance characteristics. *IEEE Trans. Power Electron.* **2019**, *34*, 10341-10358.

[15] Zhang, L.; Shi, D.; Yang, T.; Wang, K.; Tang, Y.; Loh, W.K. Split dc-bus capacitance reduction for three-phase-four-wire T-type inverter by employing power decoupling network. *IEEE Trans. Ind. Electron.* **2021**, 10.1109/TIE.2021.3073358.

[16] Xiao, Y.Y.; Du, Z.-X.; Zhang, X.Y. High-efficiency rectifier with wide input power range based on power recycling. *IEEE Trans. Circuits-II* **2018**, *65*, 744-748.

[17] Lin, W.; Zhao, Y.; Wen, G. Power transmission by microwave-a propulsion for modernization construction. *Sci. Technol. Rev.* **1994**, 31-34.

[18] Johnson, R. *Antenna engineering handbook*, 2nd ed.; McGraw-Hill, Inc.: New York, NY, 1984;

[19] Boaventura, A.; Belo, D.; Fernandes, R.; Collado, A.; Georgiadis, A.; Carvalho, N.B. Boosting the efficiency: Unconventional waveform design for efficient wireless power transfer. *IEEE Microw. Mag.* **2015**, *16*, 87-96.